Progress In Electromagnetics Research C, Vol. 22, 151–163, 2011

LOW CORRELATION MIMO ANTENNAS WITH NEGATIVE GROUP DELAY

J.-Y. Chung*, T. Yang, and J. Y. Lee

DMC R&D Center, Samsung Electronics, 416 Maetan 3-dong, Suwon, South Korea

Abstract—A key feature of upcoming 4G wireless communication systems is multiple-input-multiple-output (MIMO) technology. To make the best use of MIMO, the antenna correlation between adjacent antennas should be low (< 0.5). In this context, we propose a correlation reduction technique suitable for closely spaced antennas (distance, $d < \lambda/40$). This technique reduces mutual coupling between antennas and concurrently uncorrelates antennas' radiation characteristics by inducing the negative group delay at the target frequency. The validity of the technique is demonstrated with a USB dongle MIMO antenna designed for LTE 700 MHz band. Measurement results show that the antenna correlation is reduced more than 40% using the proposed technique.

1. INTRODUCTION

The world's leading companies in mobile communications have given a huge impetus to the development of 4G wireless systems to satisfy customers' demand for high data rate service. One of the key features enabling 4G is MIMO technology. Using multiple antennas at both the transmitter and receiver offers enhanced diversity and parallel data transfer for fast and reliable communication [1].

The best MIMO performance is achieved when data channels are uncorrelated to each other. In reality, however, it is impossible to avoid the channel correlation due to multi-path fading along the propagation channel and antenna correlation between antennas. While several adaptive signal processing techniques exist to compensate such impairments, managing low antenna correlation is rather challenging, especially for MIMO antennas implemented in a limited space.

Received 10 May 2011, Accepted 24 June 2011, Scheduled 30 June 2011

* Corresponding author: Jae-Young Chung (jay799@gmail.com).

The acceptable antenna correlation for reliable MIMO performance is reported to be < 0.5 [2]. Meeting this criterion may not be challenging for a base station MIMO antenna. On the contrary, for a MIMO antenna in a small commercial handset, the antenna correlation is inherently high as closely packed antennas are strongly coupled to each other. Such problem is more critical for the lower frequency range (e.g., E-UTRA LTE band 17, 704–746 MHz), as the wavelength is longer and antennas are electrically closer.

While a number of techniques have been proposed to reduce the antenna correlation, only few are available for small commercial handsets operating at the lower frequency range. The most popular correlation reduction technique is enforcing spatial or polarization diversity by mechanically separating or rotating the antennas [3–5]. However, this may not be available for small handsets due to the interference with neighboring components. Electromagnetic bandgap structures [6, 7] and defected ground structures [8, 9] have been proposed to reduce mutual coupling by suppressing the surface wave on the common ground. In spite of their effectiveness, they are impractical for commercial handsets since modifying the ground (i.e., circuit board) is not an option. It has been reported that embedded hybrid couplers [10, 11] and parasitic coupling structures [12, 13] provide low antenna correlation by decoupling the currents on the antenna elements, but they also require additional space for realization. A similar decoupling effect can be brought by connecting antennas with a suspended neutralization strip [14, 15]. Nevertheless, laborious numerical simulations are often involved to find the optimal connecting point, shape, and length of the suspended line.

In this paper, we propose a decoupling technique that significantly reduces the antenna correlation. We call it the negative group delay (NGD) technique since it enhances the isolation between antennas using NGD phenomenon. Fig. 1 illustrates a USB dongle MIMO antenna with the proposed technique. The ports of the closely packed meander antenna pair (distance, $d < 1\,\text{cm}$ or $\lambda/40$ at 740 MHz) are connected with a coupled line to induce NGD at the operation frequency. As the proposed technique electrically isolates the antennas, there is no need to physically separate them. Also, thanks to its simple structure, it is not necessary to modify the ground and/or perform extensive simulations. In Sections 2 and 3, we exploit the effect of NGD on MIMO antenna's transmission and radiation characteristics to understand its correlation reduction mechanism. Section 4 describes parametric studies by means of varying antenna's structural parameters and comparing its impact on measured data.

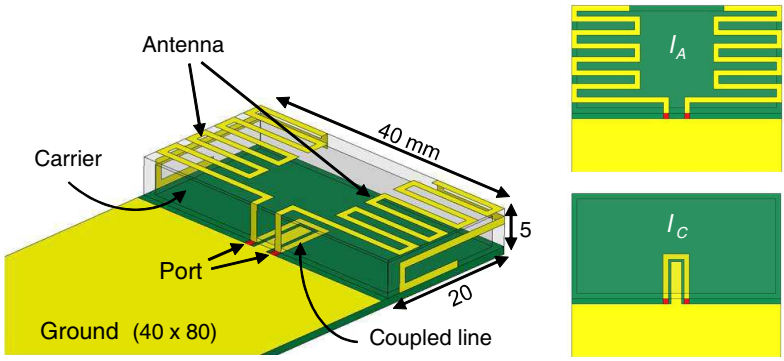

Figure 1. MIMO antenna with the proposed correlation reduction technique: (a) 3D picture and (b) 2D picture. l_A and l_C correspond to the length of the antenna and coupled line, respectively.

2. NGD FOR MIMO ANTENNAS

In a non-dispersive system (or media), the group delay is positive and constant with frequency. However, in a highly dispersive system, the group delay can be negative at a certain frequency range. Some describe this phenomenon as "superluminal propagation", implying the group velocity in the system is greater than the speed of light [16–18]. Contrarily, the opposing part claims that NGD is no other than the result of excessive phase shift or waveform dispersion [19, 20]. Although the theory behind NGD is open to dispute, its usefulness demonstrated in several applications [21–23] is unquestionable. One of the wave characteristics carried out by NGD is strong attenuation of the transmitting energy. On that account, our scope is to induce NGD and hence suppress the mutual coupling between antennas.

From a circuit perspective, NGD can be induced by loading RLC elements on a transmission line [17]. As depicted in Fig. 2, if we consider the strongly coupled antennas as a lossy transmission line, adding a coupled line emulating RLC elements may induce NGD. A study of appropriate coupled line design will be presented later. In Fig. 3, we first present the effect of NGD on MIMO antenna's transmission responses. The comparison made here is measured and simulated data of the meander antenna pair with and without the coupled line (see Fig. 1). Note that the lengths of the antenna and coupled line are $l_A = 124\,\text{mm}$ and $l_C = 20\,\text{mm}$, respectively, optimized

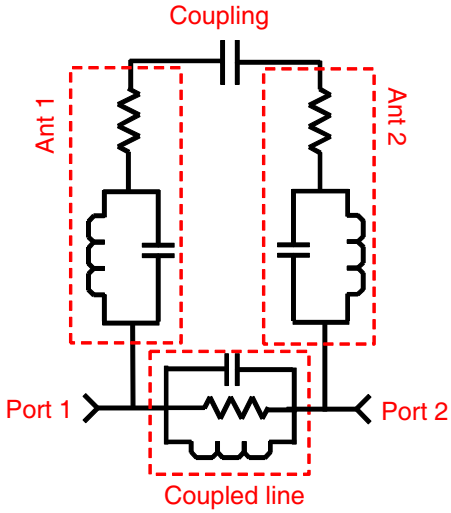

Figure 2. Equivalent circuit of a MIMO antenna with the proposed technique.

to operate at 740 MHz. As can be seen in Fig. 3(a), the S_{21} phase of the antenna without the coupled line linearly decreases as the frequency increases. On the other hand, the antenna with the coupled line shows an unusual overturn at 740 MHz. This means the group delay becomes negative at that frequency as shown in Fig. 3(b). Such NGD response is accompanied by an effective stopband characteristic, similar to an electromagnetic bandgap structure (EBG). More specifically, the difference of phase between the two wave paths from port 1 to 2 leads to destructive interference (i.e., in-phase reflection) at a certain frequency and appears as the NGD phenomenon. The dramatic drop of mutual coupling in Fig. 3(c) corresponds to this stopband characteristic. Consequently, the antenna correlation measured in a reverberation chamber [24] presents a low value of 0.35 around 740 MHz (see Fig. 3(d)). Compared to the ordinary meander antenna pair (without coupled line), this is more than 40% reduction. We note that the measured antenna correlation in Fig. 3(d) is somewhat higher than that of the simulation data from Ansoft HFSS. Such difference was caused by the radiation from unbalanced coaxial cables used in the reverberation chamber measurements. Also, the absence of data below 700 MHz in Fig. 3(d) is due to the measurable frequency limit of the reverberation chamber.

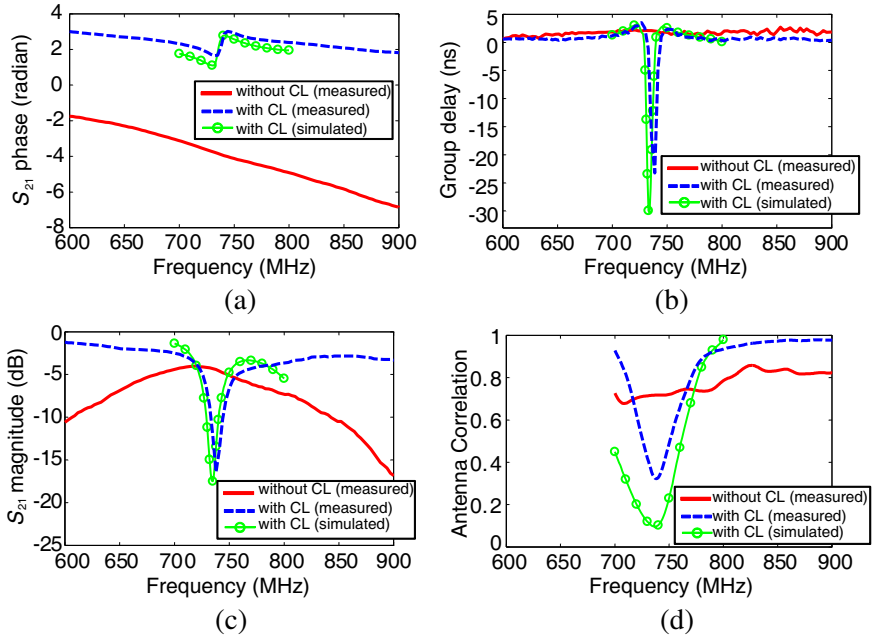

Figure 3. Measured and simulated data of the meander antenna pair with and without the coupled line: (a) S_{21} phase, (b) group delay, (c) S_{21} magnitude, and (d) antenna correlation.

3. RADIATION CHARACTERISTICS

In the previous section, the S_{21} analysis demonstrated that NGD results in the reduction of antenna correlation via minimizing the mutual coupling. Meanwhile, it is important to examine MIMO antenna's far-field radiation patterns as the antenna correlation is calculated from their inner product. That is,

$$\begin{aligned}\rho &= \frac{\left|\oint \mathbf{E_1}\cdot\mathbf{E_2}^{*}\mathbf{d\Omega}\right|^2}{\left|\oint \mathbf{E_1}\cdot\mathbf{E_1}^{*}\mathbf{d\Omega}\times\oint \mathbf{E_2}\cdot\mathbf{E_2}^{*}\mathbf{d\Omega}\right|} \\ &= \frac{\left|\oint E_{\theta 1}(\Omega)\,E^{*}_{\theta 2}(\Omega)+E_{\phi 1}(\Omega)\,E^{*}_{\phi 2}(\Omega)\,d\Omega\right|^2}{\left|\oint E_{\theta 1}(\Omega)\,E^{*}_{\theta 1}(\Omega)+E_{\phi 1}(\Omega)\,E^{*}_{\phi 1}(\Omega)\,d\Omega\right.} \\ &\quad \left.\times\oint E_{\theta 2}(\Omega)\,E^{*}_{\theta 2}(\Omega)+E_{\phi 2}(\Omega)\,E^{*}_{\phi 2}(\Omega)\,d\Omega\right|},\end{aligned} \tag{1}$$

where $\Omega = \sin\theta d\theta d\phi$ is the beam solid angle, and the subscript corresponds to θ (or ϕ) component of the antenna 1 (or 2) radiation

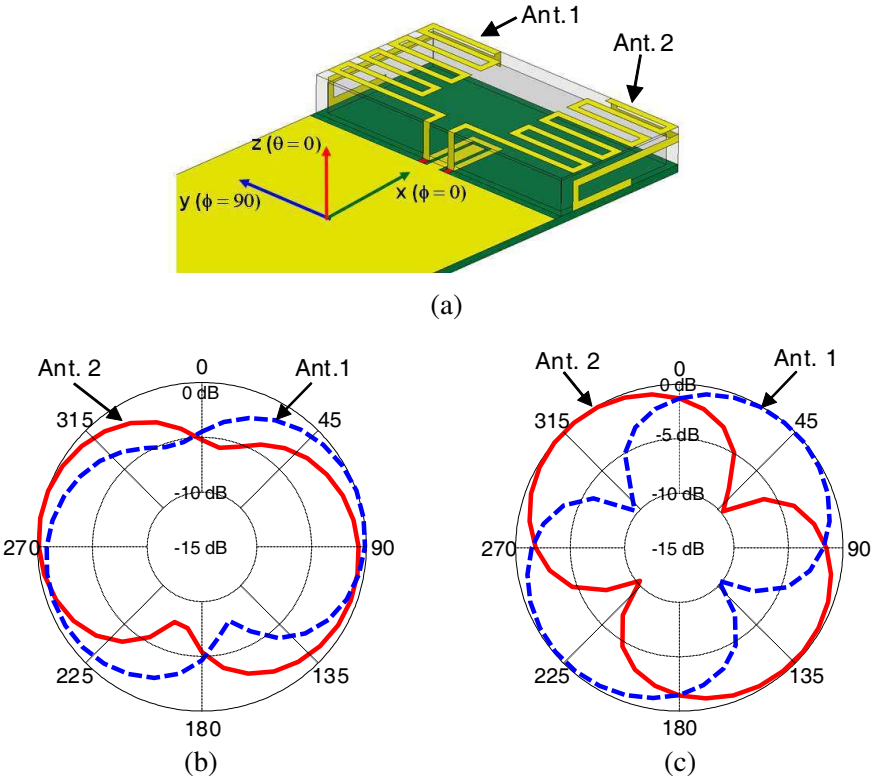

Figure 4. Far-field radiation patterns: (a) illustration of the coordinate convention, (b) patterns of the meander antenna pair without the coupled line, and (c) with the coupled line (NGD).

pattern. The numerator of (1) gives intuitive explanation of which low antenna correlation is led by pattern or polarization diversity.

Figures 4(b) and (c) are far-field radiation patterns of the MIMO antenna without and with the proposed NGD technique, respectively. More specifically, they are E_θ components along the xy-plane carried out using Ansoft HFSS with the set-up depicted in Fig. 4(a). The measurement data from an anechoic chamber show similar patterns but are not included for clarity. As observed in Fig. 4(c), the antenna patterns are orthogonal to each other when NGD is induced by connecting two antennas with the coupled line. This implies that NGD results in decoupling of two orthogonal radiation modes. Subsequently, the numerator of (1) becomes small as the peaks of one antenna overlap with the nulls of the other. Otherwise, the patterns of the antenna pair

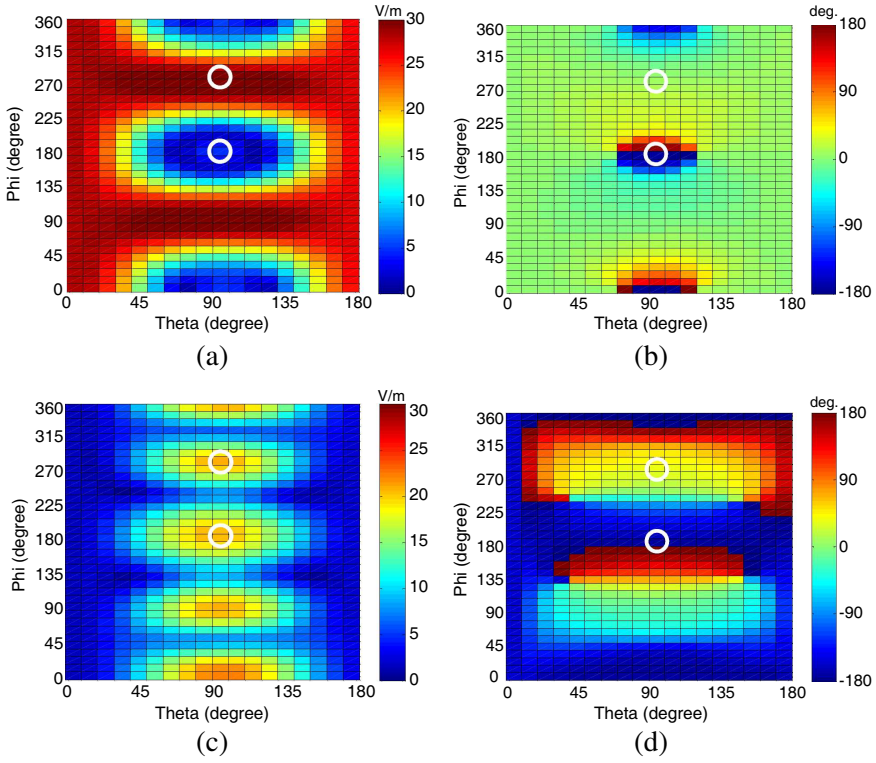

Figure 5. Values of $A(\theta, \phi)$ at different angles: (a) magnitude for the antenna without the coupled line, (b) phase without the coupled line, (c) magnitude with the couple line, and (d) phase with the coupled line.

without the coupled line (see Fig. 4(b)) exhibit little diverseness leading to a high correlation.

The above-mentioned diversity scheme also promotes out-of-phase cancellation in the course of integration in (1). This is described in Fig. 5, which is the magnitude and phase of the integrand in the numerator of (1):

$$A(\theta, \phi) = E_{\theta 1}(\theta, \phi) E^*_{\theta 2}(\theta, \phi) + E_{\phi 1}(\theta, \phi) E^*_{\phi 2}(\theta, \phi) \quad (2)$$

Inversely, the addition of each $A(\theta, \phi)$ (i.e., cell value in Fig. 5) results to the numerator of (1). Figs. 5(a) and (b) are the magnitude and phase of (2) for the antenna without the coupled line. In contrast, Figs. 5(c) and (d) are those with the coupled line. It is clearly seen by comparison that the latter has more combinations of out-of-phase

cancelation when the cells are added. For example, the two circles in Figs. 5(c) and (d) are out-of-phase with comparable magnitude, therefore, nearly complete cancelation can be achieved by adding them. However, for the circles in Figs. 5(a) and (b), although they are out-of-phase, only a small amount of cancelation occurs since their magnitudes exhibit a great difference. As a result, the numerator of (1) with the coupled line is almost 10 times smaller than that of without the coupled line, while the denominators have the same order of magnitude.

4. PARAMETRIC STUDY

In this section, we discuss the effect of tuning geometrical parameters on MIMO antenna performances such as the operation frequency, efficiency and bandwidth.

4.1. Operation Frequency

The lengths of the antenna (l_A) and coupled line (l_C) are two crucial parameters that determine the operation frequency where NGD is induced. To evaluate this, we observed the measured S_{21} and antenna correlation with various l_A and l_C values. Figs. 6(a) and (b) show that the operation frequency shifts to lower values with increasing l_A (while l_C is fixed to 20 mm). Also, as in Figs. 6(c) and (d), the increase of l_C lowers the operation frequency (while l_A is fixed to 124 mm). Comparison of the S_{21} with the correlation values indicate that the lower S_{21} level does not necessarily result in lower antenna correlation. Although they are closely related, the antenna correlation indicates the degree of similarity in the radiation patterns, instead of the port isolation, as illustrated in the previous section. It is also found by empirical studies that the lowest antenna correlation is achieved when the length of the coupled line is around 0.05λ of the antenna resonance wavelength. Therefore, if the proposed technique is considered in MIMO antenna design, we recommend setting the coupled line length to 0.05λ first and then optimizing via further tuning.

4.2. Efficiency and Bandwidth

It is known that high antenna coupling causes degradation of antenna's total radiation efficiency due to power dissipation in the proximate radiator. This implies not only the S_{11} but S_{21} affect the efficiency of a two-port MIMO antenna.

To examine this in the proposed technique, we prepared two MIMO antennas exhibiting different S_{11} and S_{22} values. Fig. 7 shows

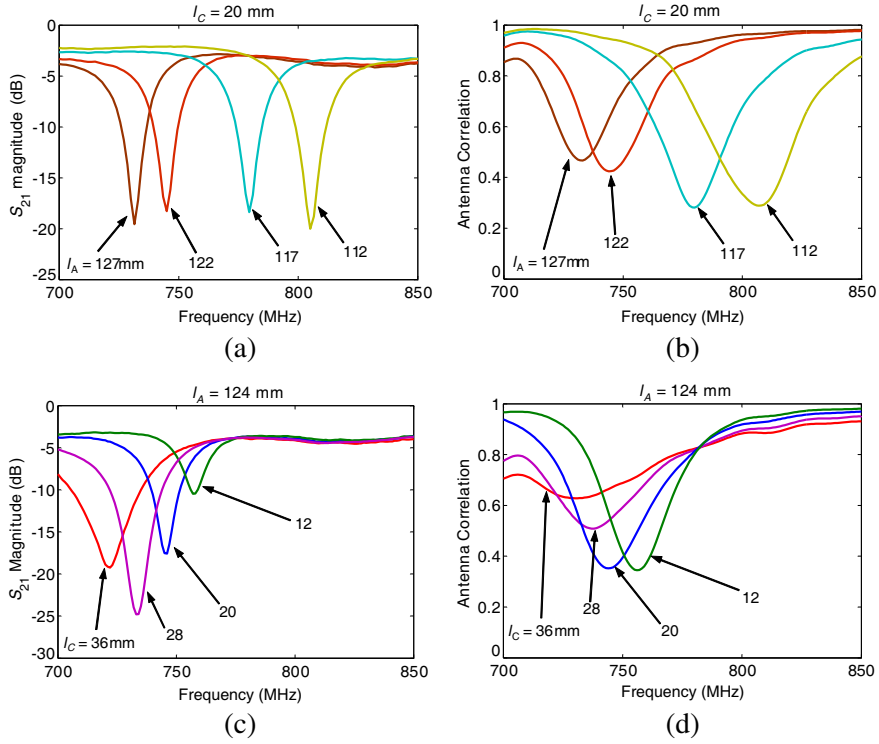

Figure 6. Measured results by varying the length of the antenna (l_A) and coupled line (l_C): (a) S_{21} magnitude with various l_A, (b) antenna correlation with various l_A, (c) S_{21} magnitude with various l_C, and (d) antenna correlation with various l_C.

the measured S-parameters of the two antennas. Here, the S_{11} and S_{21} were tuned by changing the width, gap, and length of the coupled line while sharing the same meander antennas. More specifically, the coupled line 2 (CL-2) was intentionally mismatched to have higher S_{11} (than CL-1) by decreasing the gap and increasing the length of the coupled line (i.e., increasing the coupled line impedance). As a result (shown in Fig. 7(b)), the S_{11} and S_{21} of the antenna with CL-2 is about 5 dB higher and 16 dB lower, respectively, than those of CL-1 at the operation frequency. Next, the total radiation efficiency and antenna correlation of these antennas were measured and the results are presented in Fig. 8. Also shown is the measured data of the antenna without any coupled line. As can be observed in Fig. 8(a), CL-2, despite its higher S_{11}, shows better and wider efficiency performance

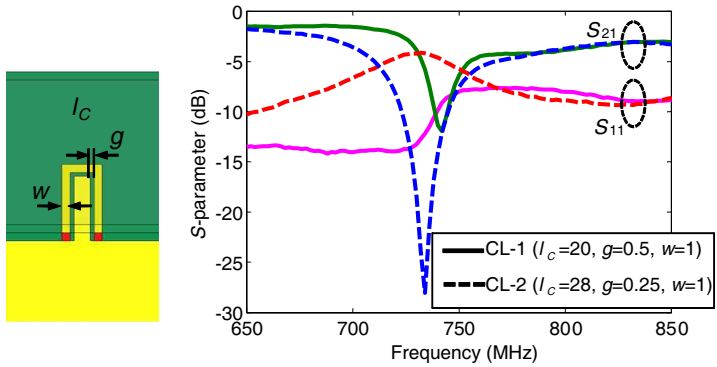

Figure 7. S-parameters with different coupled line geometries: (a) coupled line parameters and (b) measured S_{11} and S_{21}.

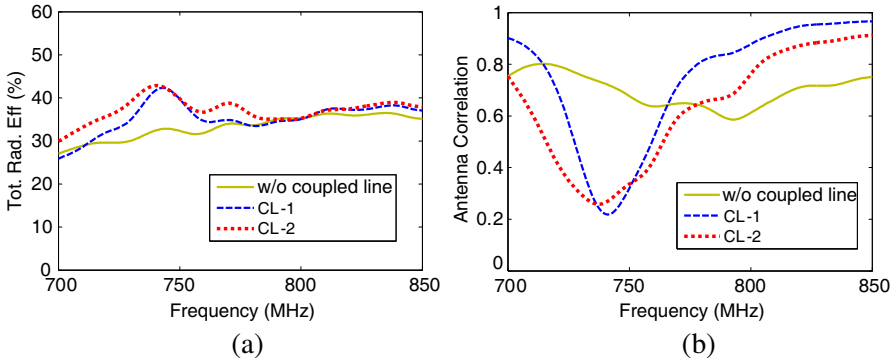

Figure 8. Comparison of MIMO antenna performance with different coupled line geometries: (a) antenna correlation and (b) total radiation efficiency.

than CL-1. This is because the remarkably low S_{21} overwhelms the impact from relatively small increase in S_{11}. The low S_{21} of CL-2 also improves the bandwidth exhibiting low correlation, as shown in Fig. 8(b). For instance, the bandwidth achieving more than 35% efficiency and less than 0.5 correlation is extended from 28 MHz to 51 MHz by tuning the coupled line from CL-1 to CL-2.

5. CONCLUSION

We presented the antenna correlation reduction technique based on novel dispersion engineering. The abnormal propagation carried out by NGD is applied to uncouple multiple antennas, which is necessary for commercial handset devices with MIMO capability. Regarding a closely packed antenna pair as a lossy transmission line, NGD could be simply induced by connecting the antenna ports with another low-loss transmission line. The study on radiation characteristics showed that extreme pattern diversity is carried out by NGD, leading to low antenna correlation. We also demonstrated the high tunability of the proposed technique by means of parametric studies. Although not included in this paper, the effectiveness of the proposed technique has been verified with different types of antennas (meander, spiral, inverted-F, etc.) at different frequency bands (LTE 13, 17, 20, etc.). Commonly, 35–44% improvement in the antenna correlation was achieved with 5–12% improvement in the total radiation efficiency. Note that such efficiency improvement is comparable to the existing suspended line technique [12, 13] but the correlation reduction is superior (about 8%).

REFERENCES

1. Sampath, H., S. Talwar, J. Tellado, V. Erceg, and A. Paulraj, "A fourth-generation MIMO-OFDM broadband wireless system: Design, performance, and field trial results," *IEEE Commun. Mag.*, Vol. 40, No. 9, 143–149, 2002.
2. Vaughan, R. G. and J. B. Andersen, "Antenna diversity in mobile communications," *IEEE Trans. Veh. Technol.*, Vol. 36, No. 4, 149–172, Nov. 1987.
3. Carrasco, H., H. D. Hristov, R. Feick, and D. Cofre, "Mutual coupling between planar inverted-F antennas," *Microwave Opt. Technol. Lett.*, Vol. 42, No. 3, 224–227, Aug. 2004.
4. Karaboikis, M., C. Soras, G. Tsachtsiris, and V. Makios, "Multi element antenna systems for diversity and MIMO terminal devices," *PIERS Proceedings*, 2004.
5. Thaysen, J. and K. Jakobsen, "Wireless systems design considerations for low antenna correlation and mutual coupling reduction in multi antenna terminals," *Eur. Trans. Telecommun.*, Vol. 18, No. 3, 319–326, Apr. 2006.
6. Yang, F. and Y. Rahmat-Samii, "Microstrip antennas integrated with electromagnetic band-gap (EBG) structures: A low mutual

coupling design for array applications," *IEEE Trans. Antennas Propag.*, Vol. 51, No. 10, 2936–2946, Oct. 2003.

7. Nashaat Elsheakh, D. N., M. F. Iskander, E. A.-F. Abdallah, H. A. Elsadek, and H. Elhenawy, "Microstrip array antenna with new 2D-electromagnetic band gap structure shapes to reduce harmonics and mutual coupling," *Progress In Electromagnetics Research C*, Vol. 12, 203–213, 2010.
8. Chung, Y., S. S. Jeon, D. Ahn, J. I. Choi, and T. Itoh, "High isolation dual-polarized patch antenna using defected ground structure," *IEEE Microw. Wireless Compon. Lett.*, Vol. 14, No. 1, 4–6, 2004.
9. Chiu, C.-Y., C.-H. Cheng, R. D. Murch, and C. R. Rowell, "Reduction of mutual coupling between closely-packed antenna elements," *IEEE Trans. Antennas Propag.*, Vol. 55, No. 6, 1732–1738, Jun. 2007.
10. Chen, S.-C., Y.-S. Wang, and S.-J. Chung, "A decoupling technique for increasing the port isolation between two strongly coupled antennas," *IEEE Trans. Antennas Propag.*, Vol. 56, No. 12, 3650–3658, Dec. 2008.
11. Bhatti, R. A., S. Yi, and S. Park, "Compact antenna array with port decoupling for LTE-standardized mobile phones," *IEEE Antennas Wireless Propag. Lett.*, Vol. 8, 430–1433, 2009.
12. Mak, A. C. K., C. R. Rowell, and R. D. Murch, "Isolation enhancement between two closely packed antennas," *IEEE Trans. Antennas Propag.*, Vol. 56, No. 11, 3411–3419, Nov. 2008.
13. Li, C., S. Chen, and P. Hsu, "Integrated dual planar inverted-F antenna with enhanced isolation," *IEEE Antennas Wireless Propag. Lett.*, Vol. 8, 963–965, 2009.
14. Diallo, A., C. Luxey, P. L. Thuc, R. Staraj, and G. Kossiavas, "Study and reduction of the mutual coupling between two mobile phone PIFAs operating in the DCS1800 and UMTS bands," *IEEE Trans. Antennas Propag.*, Vol. 54, No. 11, 3063–3074, Nov. 2006.
15. Chiu, C.-W., C.-H. Chang, and Y.-J. Chi, "A meandered loop antenna for LTE/WWAN operations in a smart phone," *Progress In Electromagnetics Research C*, Vol. 16, 147–160, 2010.
16. Bolda, E. L., R. Y. Chiao, and J. C. Garrison, "Two theorems for the group velocity in dispersive media," *Phys. Rev. A*, Vol. 48, No. 5, 3890–3894, 1993.
17. Siddiqui, O. F., M. Mojahedi, and G. V. Eleftheriades, "Periodically loaded transmission line with effective negative refractive index and negative goup delay," *IEEE Trans. Antennas*

Propag., Vol. 51, No. 10, 2619–2625, 2003.

18. Withayachumnankul, W., B. M. Fischer, B. Ferguson, B. R. Davis, and D. Abbott, "A systemized view of superluminal wave propagation," *Proc. IEEE*, Vol. 98, No. 10, 1775–1786, Oct. 2010.
19. Stenlus, P. and B. York, "On the propagation of transients in waveguides," *IEEE Antennas and Propag. Mag.*, Vol. 37, No. 2, 39–44, Apr. 1995.
20. Cripps, S. C., "Waving back," *IEEE Microwave Mag.*, Vol. 11, No. 2, 20–32, Apr. 2010.
21. Siddiqui, O. F., S. J. Erickson, G. V. Eleftheriades, and M. Mojahedi, "Time domain measurement of negative group delay in negative refractive index transmission line metamaterials," *IEEE Trans. Microw. Theory Tech.*, Vol. 52, No. 5, 1449–1454, May 2004.
22. Ravelo, B., A. Perennec, M. Le Roy, and Y. Boucher, "Active microwave circuit with negative group delay," *IEEE Microw. Wireless Compon. Lett.*, Vol. 17, No. 12, 861–863, Dec. 2007.
23. Choi, H., Y. Jeong, C. D. Kim, and J. S. Kenney, "Efficiency enhancement of feedforward amplifiers by employing a negative group-delay circuit," *IEEE Trans. Microw. Theory Tech.*, Vol. 58, No. 5, 1116–1125, May 2010.
24. Kildal, P. S. and K. Rosengren, "Correlation and capacity of MIMO systems and mutual coupling, radiation efficiency, and diversity gain of their antennas: Simulations and measurements in a reverberation chamber," *IEEE Commun. Mag.*, Vol. 42, 104–112, 2004.